



Optimization and SAR research at the piperazine and phenyl rings of JNJ4796 as new anti-influenza A virus agents, part 1



Aoyu Wang^{a,b}, Yuhuan Li^a, Kai Lv^{a,*}, Rongmei Gao^a, Apeng Wang^a, Haiyan Yan^a, Xiaoyu Qin^a, Shijie Xu^a, Chao Ma^a, Jiandong Jiang^a, Zengquan Wei^c, Kai Zhang^{b,**}, Mingliang Liu^{a,***}

^a CAMS Key Laboratory of Antiviral Drug Research, Beijing Key Laboratory of Antimicrobial Agents, NHC Key Laboratory of Biotechnology of Antibiotics, Institute of Medicinal Biotechnology, Chinese Academy of Medical Sciences and Peking Union Medical College, Beijing, 100050, China

^b Department of Pharmaceutical Chemistry, School of Pharmacy, Hebei Medical University, Shijiazhuang, 050017, China

^c Chemical Medicine Department, R&D Center, Tasly Pharmaceutical Group Co. Ltd., Tianjin, 300410, China

ARTICLE INFO

Article history:

Received 20 March 2021

Received in revised form

24 May 2021

Accepted 26 May 2021

Keywords:

Influenza A virus

JNJ4796

Hemagglutinin inhibitors

Structure-activity relationship

ABSTRACT

JNJ4796, a small molecule fuse inhibitor targeting the conserved stem region of hemagglutinin, effectively neutralized a broad spectrum of group 1 influenza A virus (IAV), and protected mice against lethal and sublethal influenza challenge after oral administration. In this study, we reported the modification and structure-activity relationship (SAR) of C (piperazine ring) and E (phenyl ring) rings of JNJ4796. Compound (**R**)-**2c** was identified to show excellent *in vitro* activity against IAV H1N1 and Oseltamivir-resistant IAV H1N1 stains (IC₅₀: 0.03–0.06 μM), low cytotoxicity (CC₅₀ > 200 μM), accepted oral PK profiles and low inhibition rate of hERG (13.2%, at 10 μM). Evaluation for the *in vivo* anti-IAV efficacy of (**R**)-**2c** will begin soon.

© 2021 Elsevier Masson SAS. All rights reserved.

1. Introduction

Influenza A virus (IAV), an enveloped negative-sense RNA virus belongs to the orthomyxoviridae family, can cause substantial morbidity and mortality through seasonal epidemics [1,2]. The World Health Organization (WHO) estimated that approximately 5–10% of adults and 20–30% of children infected annually, 3–5 million cases of severe diseases and 250,000–500,000 deaths occur from influenza each year worldwide [3]. Seasonal influenza vaccinations remain the principal prophylactic for controlling influenza infections, but the efficacy is limited by the rapid antigenic drift and shift in influenza viruses [4,5]. To date, three classes of anti-influenza drugs are available on the market. The influenza M2 ion channel blockers (Amantadine and Rimantadine) are not recommended anymore since all of the circulating influenza strains are resistant to them [9,10]. The neuraminidase inhibitors (NAIs)

Oseltamivir, Zanamivir, and Peramivir (Fig. 1) [6,7], as well as the most recently developed polymerase acidic (PA) protein inhibitor Baloxavir (Fig. 1) [8], are major therapeutic options for new influenza outbreaks. Unfortunately, NAIs- and Baloxavir-resistant strains also have been reported [11–14]. Thus, there is a pressing and urgent unmet need for new broad-spectrum influenza antivirals to suppress seasonal and pandemic influenza.

IAV has two surface glycoproteins, hemagglutinin (HA) and neuraminidase (NA). Based on the antigenicity of HA and NA, IAV has been classified into 18 hemagglutinin subtypes (H1 to H18) and 11 neuraminidase subtypes (N1 to N11) [15]. HA subtypes are further divided phylogenetically into two groups (Group 1: H1, H2, H5, H6, H8, H9, H11, H12, H13, H16, H17 and H18; Group 2: H3, H4, H7, H10, H14 and H15) [16]. The conserved stem region of HA has been recently recognized as a potential anti-IAV target to develop broad spectrum inhibitors [17,18]. Through high-throughput screening and optimization, scientists from Janssen Pharma and Scripps Institute collaboratively discovered JNJ4796 (Fig. 2), a small molecule targeting the conserved stem region of HA, effectively neutralized a broad spectrum of group 1 IAV (H1, H2, H5, H6, H11, H13 and H16) *in vitro*. In addition, twice daily oral administration of JNJ4796 (5 mg/kg) in the H1N1 infection mouse model gave rise to 100% survival and only moderate weight loss effects [18].

* Corresponding author.

** Corresponding author.

*** Corresponding author.

E-mail addresses: Lvkaik@hotmail.com (K. Lv), zhk810728@163.com (K. Zhang), mllyx@126.com (M. Liu).

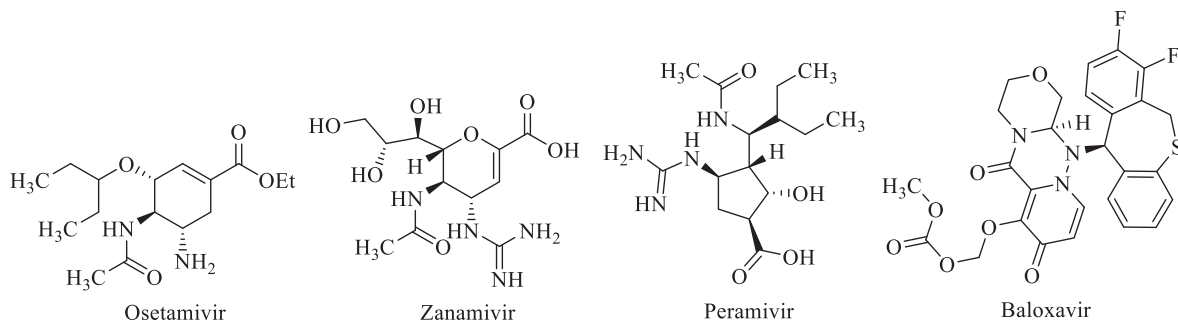


Fig. 1. Structures of anti-IAV drugs.

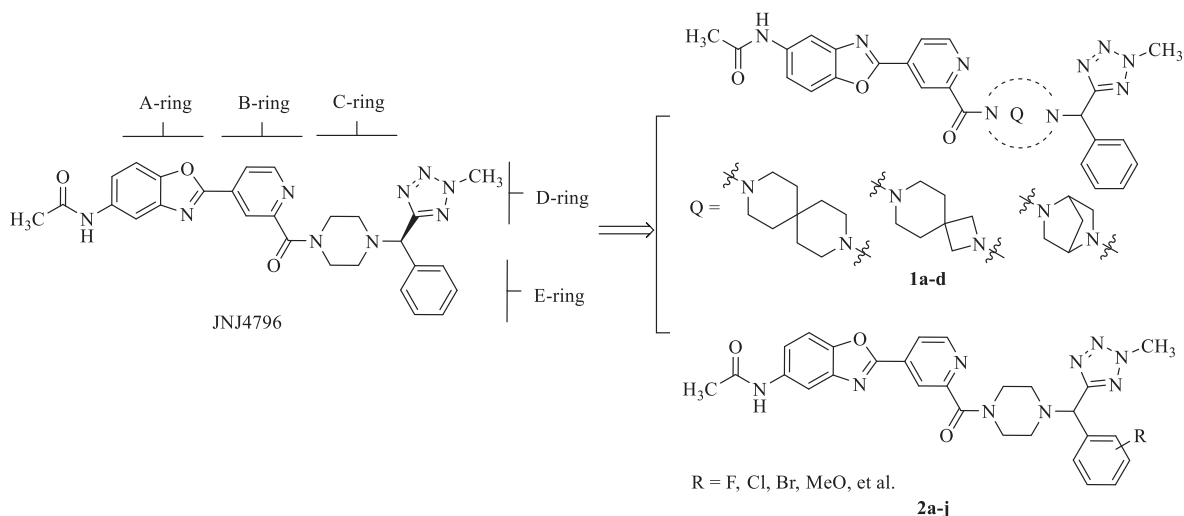


Fig. 2. Design of new target compounds.

Encouraged by the promising *anti*-IAV activity and novel mechanism of JNJ4796, we initiated an optimization campaign with the goal of identifying new HA inhibitor through systematically exploring each ring system (A-E rings) of JNJ4796. In this work, we studied the structure-activity relationship (SAR) of C (piperazine ring) and E rings (phenyl ring) of JNJ4796, optimization of the other three rings was reported in due course (Fig. 2).

In our previous studies [19–21], replacement of the piperazine ring of PBTZ169 (a known *anti*-TB candidate) with symmetrical spiro- or bridged diazaheterocycles was proved to be a successful optimization strategy. Therefore, we started with our modifications on the C ring of JNJ4796 by displacement of the piperazine with three diazaheterocycles. After identifying optimal C ring, we focused on optimization of the E ring of JNJ4796 since phenyl was prone to be metabolized by CYP450 enzyme [22–24]. Considering the fact that the phenyl group of JNJ4796 is wrapped in a small binding pocket and forms CH- π bonds with His¹⁸ from HA1 [18], only small size substituents could be accommodated into this pocket. Thus, some small substituents (such as F, Cl, Br, et al.) were introduced to the phenyl moiety (E ring) to improve metabolic stability.

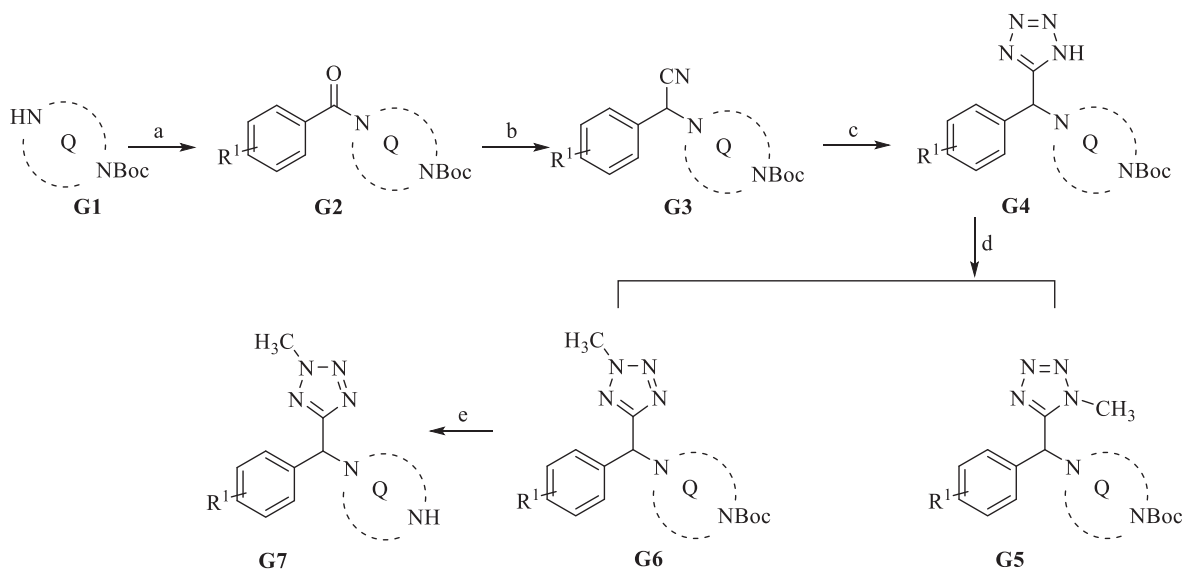
In this study, a series of JNJ4796 derivatives containing diazaheterocycles and substituted phenyls as C and E rings, respectively, were designed and synthesized. Our primary objective was to find alternative *anti*-IAV candidates with potent activity and drug-like properties. A preliminary SAR study was also explored to facilitate further development of these compounds.

2. Results and discussion

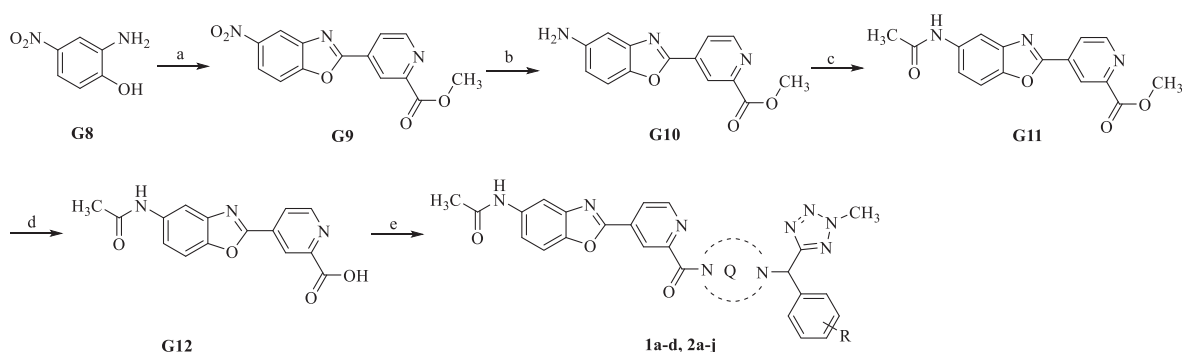
2.1. Chemistry

General synthetic routes for key intermediates **G7** and target compounds **1–2** were shown in Schemes 1 and 2, respectively. Coupling of Boc-protected cyclic amines (piperazine and diazaheterocycles) with substituted benzoic acids (R¹-PhCOOH), followed by Iridium-catalyzed reductive Strecker reaction of the resulted amides **G2** gave *α*-amino phenylacetonitriles **G3**. [3 + 2] cycloaddition of the nitriles and trimethylsilyl azide in the presence of tributyltin oxide furnished tetrazoles **G4**, which upon nucleophilic substitution with CH₃I provided a mixture of positional isomers (**G5**: **G6** ≈ 1 : 1). The two positional isomers were conveniently separated by silica gel chromatography (Rf: G5 < G6, EtOAc: Hexane = 1 : 2), but NOE and ¹H NMR failed to distinguish the two isomers. Fortunately, the single crystal of isomer **G5-2e** (Fig. 3) was successfully cultured, and the definite position of the methyl group on the tetrazole ring was thus confirmed. The key intermediates **G7** were easily prepared by removal of the Boc-group of **G6** with TFA (Scheme 1).

As shown in Scheme 2, nucleophilic addition of 2-amino-4-nitrophenol **G8** with methyl 4-formylpicolinate, followed by dehydrogenation in the presence of DDQ gave benzimidazole **G9**. The key intermediate **G12** was obtained from **G9** by catalytic hydrogenation, acetylation and hydrolysis in sequence. Finally, condensation of acid **G12** with above amines **G7** yielded the target compounds **1a-d** and **2a-j**.



Scheme 1. Synthesis of intermediates **G7**. Reagents and conditions: a): R^1 -PhCOOH, EDCl, DMAP, DCM, rt; b): $IrCl(CO)[P(C_6H_5)_3]_2$, TMS, TMSCN, anhydrous Toluene; c): Bis(tributyltin) oxide, azidotrimethylsilane, anhydrous toluene, 110 °C; d): MeI, K_2CO_3 , MeCN; e): TFA, DCM, 0 °C-rt.



Scheme 2. Synthesis of target compounds **1a-d** and **2a-j**. Reagents and conditions: a): (i) Methyl 4-formylpicolinate, MeOH, 60 °C; (ii) DDQ, DCM; b) H_2 1 atm, Pd/C, MeOH; c): acetic anhydride, DCM; d): LiOH, H_2O , THF; e): **G7**, EDCl, DMAP, DMF.

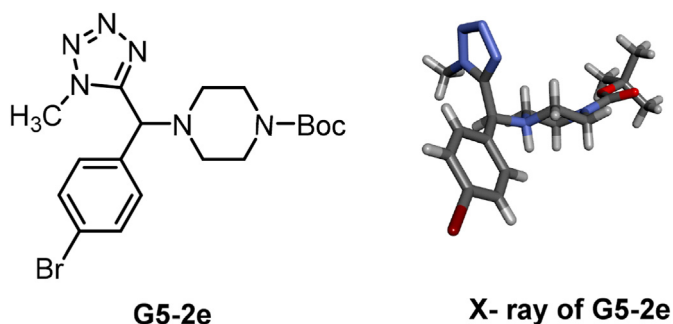


Fig. 3. Crystal structure of isomer **G5-2e**.

2.2. In vitro anti-IAV activity and cytotoxicity

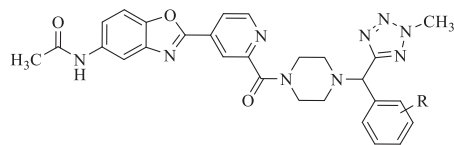
The SAR of C ring was first investigated. As shown in **Table 1**, replacement of the piperazine ring of (\pm)-JNJ4796 with three symmetrical spiro- or bridged diazaheterocycles led to significant decrease of potency (**1a-d** vs (\pm)-JNJ4796). The anti-IAV activity of compounds **1a** and **1c** were even diminished (IC_{50} : >50 μM). Yet surprisingly, compound **1d** with reversed 2,7-diazaspiro [3.5]nonane ring was active against H1N1 strain (IC_{50} : 7.41 μM), although it

Table 1

Structures, anti-IAV H1N1 activity and cytotoxicity (Series 1).

Compd.	Q	IC_{50} (μM)	CC_{50} (μM)
1a		>50	>50
1b		18.50	>50
1c		>50	>50
1d		7.41	32.05
(\pm)-JNJ4796		0.35	>50

showed slightly higher cytotoxicity against MDCK cell (CC_{50} : 32.05 μM) than compound **1c** (CC_{50} : >50 μM). These results

Table 2
Structures, *anti*-IAV H1N1 activity and cytotoxicity (Series 2).

Compd.	R	IC ₅₀ (μM)	CC ₅₀ (μM)
2a	2-F	7.41	>50
2b	3-F	2.47	>50
2c	4-F	0.27	>50
2d	4-Cl	1.71	>50
2e	4-Br	1.43	>50
2f	4-MeO	11.98	>50
2g	4-OCF ₃	3.18	>50
2h	4-Me	4.28	>50
2i	4-CF ₃	12.83	>50
2j	4-NO ₂	7.41	>50
(±)-JNJ4796	H	0.35	>50

revealed that employing the piperazine as C ring is essential for excellent activity.

The effect of substituents on phenyl ring (E ring) was then explored. Compounds **2a-c** with a fluorine atom at different positions on the phenyl ring of (±)-JNJ4796 were first synthesized. As shown in Table 2, introduction of a fluorine atom at *para*-position, as in compound **2c** (IC₅₀: 0.27 μM), resulted in an increased potency (**2c** vs (±)-JNJ4796), but the presence of the fluorine atom at *ortho*- and *meta*-positions (IC₅₀: 7.41 and 2.47 μM, respectively) was found to be unfavorable (**2a, b** vs (±)-JNJ4796), suggesting that the position of the substituent greatly influences activity, and the fluorine atom at *para*-is preferred over *ortho*- and *meta*-positions.

Based on above SAR, derivatives with halogens (Cl, Br), electron-donating groups (CH₃, OCH₃) or electron-withdrawing ones (CF₃, OCF₃, NO₂) at *para*-position on the phenyl ring were further designed and synthesized. Unfortunately, all of them (**2d-j**) showed decreased potency (IC₅₀: 1.43–12.83 μM). These results indicated that both the size and nature of substituent impacted the activity,

Table 3
Anti-IAV activity and cytotoxicity of (**S**)-**2c** and (**R**)-**2c**.

Compd.	CC ₅₀ ^a (μM)	IAV H1N1		Oseltamivir-resistant IAV H1N1 ^b	
		IC ₅₀ (μM) ^a	SI	IC ₅₀ (μM) ^a	SI
(S)- 2c	>200	5.51 ± 1.74	>36	6.65 ± 1.31	>30
(R)- 2c	>200	0.03 ± 0.05	>6666	0.06 ± 0.02	>3333
(S)-JNJ4796	>200	1.90 ± 0.18	>105	8.50 ± 1.89	>23
(R)-JNJ4796 (JNJ4796)	143.65 ± 48.80	0.04 ± 0.04	3591	0.05 ± 0.02	2873
Ribavirin	>200	4.28 ± 0.00	>46	4.28 ± 0.00	>46
Oseltamivir	>200	3.44 ± 0.84	>58	179.56 ± 35.41	>1

^a The cytotoxicity and anti-virus activity were tested for 3 times.

^b Oseltamivir-resistant IAV H1N1 (clinical isolated IAV/Tianjin Jinnan/15/2009) was kindly provided by Professor Yuelong Shu at the Institute for Viral Disease Control and Prevention, China Centers for Disease Control and Prevention, Beijing, China.

Table 4
Further appraisal of (**R**)-**2c** and JNJ4796.

Compd.	Pharmacokinetic profiles ^a				hERG IR ^b (n = 3)
	T _{1/2} (h)	T _{max} (h)	C _{max} (ng·mL ⁻¹)	AUC _{0-inf} (h·ng·mL ⁻¹)	
(R)- 2c	5.84 ± 0.63	0.33 ± 0	866 ± 205	1913 ± 554	13.2 ± 2.87%
JNJ4796	3.69 ± 0.60	0.25 ± 0	572 ± 166	1214 ± 561	53.8 ± 4.04%

^a Pharmacokinetic properties in Balb/c mice after a single oral administration of 25 mg/kg, n = 3.

^b hERG K⁺ channel inhibition rate at 10 μM, n = 3. Abbreviations: t_{1/2}, elimination half-life; T_{max}, the time at which the C_{max} is observed; C_{max}, the maximum serum concentration; AUC_{0-inf}, area under the concentration-time curve up to infinite time; hERG, human Ether-a-gogo related gene.

which is consistent with the analysis result of binding pattern as we mentioned above.

In order to determine influence of the chiral center to *anti*-IAV activity, we conducted chiral separation of the most potent compound **2c**. The absolute configurations of two enantiomers were confirmed by ECD spectrum (Fig. S1.), and optical rotations were measured. The two enantiomers were evaluated for their *anti*-IAV activity against IAV H1N1 and Oseltamivir-resistant IAV H1N1 strains along with JNJ4796, Ribavirin and Oseltamivir for comparison. As shown in Table 3, The two enantiomers displayed potent *anti*-IAV activity against both of IAV H1N1 (IC₅₀: 0.03–5.51 μM) and Oseltamivir resistant-IAV H1N1 strains (IC₅₀: 0.06–6.65 μM). The enantiomer (**R**)-**2c** (IC₅₀: 0.03–0.06 μM) was found to be much more active than (**S**)-**2c** (IC₅₀: 5.51–6.65 μM), indicating the *anti*-IAV activity of **2c** is the same enantioselective as (±)-JNJ4796 (Table 2). Moreover, it is worth to note that (**R**)-**2c** showed lower cytotoxicity (CC₅₀ > 200 μM) and higher selective index than JNJ4796.

2.3. Further appraisal of compound (**R**)-**2c**

Subsequently, enantiomer (**R**)-**2c** was evaluated for its *in vivo* PK profiles in Balb/c mice after a single oral administration of 25 mg/kg. As shown in Table 3, (**R**)-**2c** displayed better drug exposures (C_{max}: 866 ng/mL, AUC_{0-inf}: 1913 h ng/mL), and longer half-life (T_{1/2}: 5.84 h) than JNJ4796, indicating that introduction of a fluorine atom to phenyl group (C ring) led to an improvement in metabolic stability as we originally speculated.

In most cases, compounds with high affinity for hERG ion channel can induce QT interval prolongation frequently associated with potentially lethal arrhythmias [25]. Therefore, compounds (**R**)-**2c** and JNJ4796 were further examined for their hERG inhibition rates (IRs) at 10 μM. To our delight, the IR of (**R**)-**2c** (13.2%) was significantly lower than that of JNJ4796 (Table 4).

2.4. Molecule docking study of compound (**R**)-**2c**

We predicted the binding mode of compound (**R**)-**2c** in the HA1-HA2 interface (PDB code: 6CF7) through molecular docking with

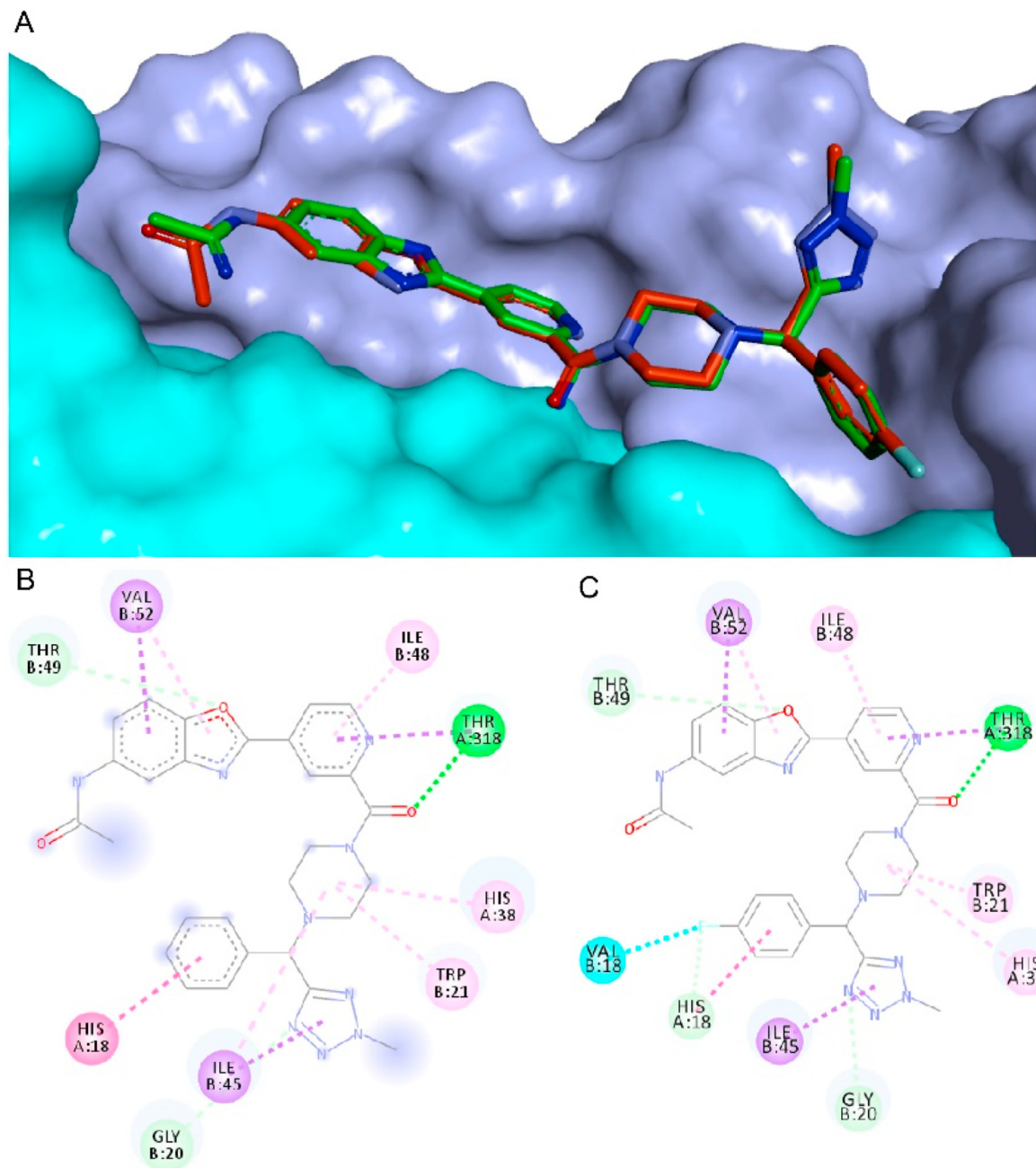


Fig. 4. Binding mode of compound (**R**)-**2c** in complex with HA: (A) comparison of the predicted binding model of compound (**R**)-**2c** and JNJ4796 in the HA X-ray structure (PDB code: 6CF7), surface of HA1 is in blue color, surface of HA2 is in cyan color, carbons of JNJ4796 are in green color, carbons of (**R**)-**2c** are in red color; (B) The detailed interactions between JNJ4796 and HA1-HA2 interface; (C) The predicted interactions between compound (**R**)-**2c** and HA1-HA2 interface.

CDOCK module of Discovery Studio 3.5. The docked model of the compound (**R**)-**2c** was compared with JNJ4796 which is an intrinsic ligand from the X-ray structure (PDB code: 6CF7). As the chemical structure of compound (**R**)-**2c** was similar to JNJ4796, the binding model of compound (**R**)-**2c** also showed a closed interaction pattern with JNJ4796 (Fig. 4A). The ligand-receptor interaction analysis showed that the binding site of (**R**)-**2c** and JNJ4796 comprised similar residues (Thr49, Val 52, Ile 48, Thr318, Ile 45, His 38, Trp 21, Gly 20 and His18) (Fig. 4B and C). Notably, the fluorenyl moiety of (**R**)-**2c** could be adjusted into the small binding pocket, and the fluorine atom interacted with His18 and Val 18, which may enhance the binding affinity. In contrast, compounds **2d-j** with Cl, Br or Me et al. substituents may experience steric clashes and led to reduced activity.

3. Conclusion

In summary, two series of JNJ4796 analogues were synthesized and evaluated for their *anti*-IAV activity. Replacement of the piperazine ring with spiro- or bridged diazaheterocycles resulted in a dramatically decreased potency, suggesting that the piperazine ring is an irreplaceable portion and essential for ligand-target interactions. Introduction of substituents to the phenyl ring of JNJ4796 was also detrimental, and the only exception is 4-fluorenyl analogue **2c** (IC_{50} : 0.27 μ M) with better potency (IC_{50} : 0.27 μ M) than (\pm)-JNJ4796 (IC_{50} : 0.35 μ M).

The racemic **2c** was then resolved via Chiral preparation-HPLC. The absolute configurations of enantiomers were confirmed by ECD spectrum, and optical rotations were measured. Both of them

were further evaluated for their *anti*-IAV activity against IAV H1N1 and Oseltamivir-resistant IAV H1N1 stains. Enantiomer (**R**)-**2c** (IC₅₀: 0.03–0.06 μM) showed significantly higher *anti*-IAV potency than (**S**)-**2c** (IC₅₀: 5.51–6.65 μM), and comparable activity to JNJ4796 (IC₅₀: 0.04–0.05 μM). More importantly, (**R**)-**2c** displayed lower cytotoxicity (CC₅₀ > 200 μM), better oral PK profiles and significantly lower hERG IR (13.2%, at 10 μM) than JNJ4796. Studies to determine the *in vivo* *anti*-IAV efficacy of (**R**)-**2c** will begin soon.

Ethical statement

All animal experiments were carried out in accordance with the guidelines of the Chinese Association for Laboratory Animal Sciences and approved by the institutional ethical committee (IEC) of Peking Union Medical College.

Funding sources

This work is supported by CAMS Initiative for Innovative Medicine (CAMS-2018-I2M-3–004, CAMS-2020-I2M-2–010), the National Mega-project for Innovative Drugs (2018ZX09711001-007-002), Foundation of the Hebei Education Department Science Research Project (ZD2020164), Biomedicine Special Project of Hebei Province of China (20372607D).

Declaration of competing interest

The authors declare that they have no known competing financial interests or personal relationships that could have appeared to influence the work reported in this paper.

Appendix A. Supplementary data

Supplementary data to this article can be found online at <https://doi.org/10.1016/j.ejmech.2021.113591>.

References

- [1] S. Yuan, L. Wen, J. Zhou, Inhibitors of influenza A virus polymerase, *ACS Infect. Dis.* 4 (2018) 218–223.
- [2] A.J. Eisfeld, G. Neumann, Y. Kawaoka, At the centre: influenza A virus ribonucleoproteins, *Nat. Rev. Microbiol.* 13 (2015) 28–41.
- [3] World Health Organization (WHO), WHO influenza (seasonal) fact sheet. [www.who.int/en/news-room/fact-sheets/detail/influenza-\(seasonal\)](http://www.who.int/en/news-room/fact-sheets/detail/influenza-(seasonal)), 2018.
- [4] M.T. Osterholm, N.S. Kelley, A. Sommer, E.A. Belongia, Efficacy and effectiveness of influenza vaccines: a systematic review and meta-analysis, *Lancet Infect. Dis.* 12 (2012) 36–44.
- [5] K.L. Nichol, J.D. Nordin, D.B. Nelson, J.P. Mullooly, E. Hak, Effectiveness of influenza vaccine in the community-dwelling elderly, *N. Engl. J. Med.* 357 (2007) 1373–1381.
- [6] E. De Clercq, Antiviral agents active against influenza A viruses, *Nat. Rev. Drug Discov.* 5 (2006) 1015–1025.
- [7] J. Beigel, M. Bray, Current and future antiviral therapy of severe seasonal and avian influenza, *Antivir. Res.* 78 (2008) 91–102.
- [8] F.G. Hayden, N. Sugaya, N. Hirotsu, N. Lee, M.D. de Jong, A.C. Hurt, T. Ishida, H. Sekino, K. Yamada, S. Portsmouth, K. Kawaguchi, T. Shishido, M. Arai, K. Tsuchiya, T. Uehara, A. Watanabe, Baloxavir marboxil for uncomplicated influenza in adults and adolescents, *N. Engl. J. Med.* 379 (2018) 913–923.
- [9] R.A. Bright, M.-j. Medina, X. Xu, G. Perez-Orozco, T.R. Wallis, X.M. Davis, L. Povinelli, N.J. Cox, A.I. Klimov, Incidence of adamantane resistance among influenza A (H3N2) viruses isolated worldwide from 1994 to 2005: a cause for concern, *Lancet* 366 (2005) 1175–1181.
- [10] R.A. Bright, D.K. Shay, B. Shu, N.J. Cox, A.I. Klimov, Adamantane resistance among influenza A viruses isolated early during the 2005–2006 influenza season in the United States, *J. Am. Med. Assoc.* 295 (2006) 891–894.
- [11] Q.M. Le, M. Kiso, K. Someya, Y.T. Sakai, T.H. Nguyen, K.H.L. Nguyen, N.D. Pham, H.H. Ngyen, S. Yamada, Y. Muramoto, T. Horimoto, A. Takada, H. Goto, T. Suzuki, Y. Suzuki, Y. Kawaoka, Isolation of drug-resistant H5N1 virus, *Nature* 437 (2005), 1108–1108.
- [12] M.D. de Jong, T.T. Thanh, T.H. Khanh, V.M. Hien, G.J.D. Smith, N.V. Chau, B.V. Cam, P.T. Qui, D.Q. Ha, Y. Guan, J.S.M. Peiris, T.T. Hien, J. Farrar, Oseltamivir resistance during treatment of influenza A (H5N1) infection, *N. Engl. J. Med.* 353 (2005) 2667–2672.
- [13] K.A. Kormuth, S.S. Lakdawala, Emerging antiviral resistance, *Nat. Microbiol.* 5 (2020) 4–5.
- [14] M. Imai, M. Yamashita, Y. Sakai-Tagawa, K. Iwatsuki-Horimoto, M. Kiso, J. Murakami, A. Yasuhara, K. Takada, M. Ito, N. Nakajima, K. Takahashi, T.J.S. Lopes, J. Dutta, Z. Khan, D. Kriti, H. van Bakel, A. Tokita, H. Hagiwara, N. Izumida, H. Kuroki, T. Nishino, N. Wada, M. Koga, E. Adachi, D. Jubishi, H. Hasegawa, Y. Kawaoka, Influenza A variants with reduced susceptibility to baloxavir isolated from Japanese patients are fit and transmit through respiratory droplets, *Nat. Microbiol.* 5 (2020) 27–33.
- [15] Q. Zhang, T. Liang, K.S. Nandakumar, S. Liu, Emerging and state of the art hemagglutinin-targeted influenza virus inhibitors, *Expert Opin. Pharmacother.* (2020) 1–14.
- [16] S. Tong, X. Zhu, Y. Li, M. Shi, J. Zhang, M. Bourgeois, H. Yang, X. Chen, S. Recuenco, J. Gomez, L.-M. Chen, A. Johnson, Y. Tao, C. Dreyfus, W. Yu, R. McBride, P.J. Carney, A.T. Gilbert, J. Chang, Z. Guo, C.T. Davis, J.C. Paulson, J. Stevens, C.E. Rupprecht, E.C. Holmes, I.A. Wilson, R.O. Donis, New world bats harbor diverse influenza A viruses, *PLoS Pathog.* 9 (2013), e1003657.
- [17] A. Antanasijevic, M.A. Durst, H. Cheng, I.N. Gaisina, J.T. Perez, B. Manicassamy, L. Rong, A. Lavie, M. Caffrey, Structure of avian influenza hemagglutinin in complex with a small molecule entry inhibitor, *Life Sci Alliance* 3 (2020), e2022000724.
- [18] M.J.P. van Dongen, R.U. Kadam, J. Juraszek, E. Lawson, B. Brandenburg, F. Schmitz, W.B.G. Schepens, B. Stoops, H.A. van Diepen, M. Jongeneelen, C. Tang, J. Vermond, A. van Eijgen-Obregoso Real, S. Blokland, D. Garg, W. Yu, W. Goutier, E. Lanckacker, J.M. Klap, D.C.G. Peeters, J. Wu, C. Buyck, T.H.M. Jonckers, D. Roymans, P. Roevens, R. Vogels, W. Koudstaal, R.H.E. Friesen, P. Raboisson, D. Dhanak, J. Goudsmit, I.A. Wilson, A small-molecule fusion inhibitor of influenza virus is orally active in mice, *Science* 363 (2019) eaar6221.
- [19] K. Lv, X. You, B. Wang, Z. Wei, Y. Chai, B. Wang, A. Wang, G. Huang, M. Liu, Y. Lu, Identification of better pharmacokinetic benzothiazinone derivatives as new antitubercular agents, *ACS Med. Chem. Lett.* 8 (2017) 636–641.
- [20] K. Lv, A. Wang, Z. Tao, L. Fu, H. Liu, B. Wang, C. Ma, H. Wang, X. Ma, B. Han, A. Wang, K. Zhang, M. Liu, Y. Lu, hERG optimizations of IMB1603, discovery of alternative benzothiazinones as new antitubercular agents, *Eur. J. Med. Chem.* 179 (2019) 208–217.
- [21] K. Lv, S. Wu, W. Li, Y. Geng, M. Wu, J. Zhou, Y. Li, Q. Gao, M. Liu, Design, synthesis and anti-HBV activity of NVR3-778 derivatives, *Bioorg. Chem.* 94 (2020) 103363.
- [22] W. Jiang, L. Hong, Lead compound optimization strategy (1)-changing metabolic pathways and optimizing metabolism stability, *Acta Pharm. Sin.* 48 (2013) 1521–1531.
- [23] H. van de Waterbeemd, D.A. Smith, K. Beaumont, D.K. Walker, Property-based Design: optimization of drug absorption and pharmacokinetics, *J. Med. Chem.* 44 (2001) 1313–1333.
- [24] Z. Zhang, W. Tang, Drug metabolism in drug discovery and development, *Acta Pharm. Sin. B.* 8 (2018) 721–732.
- [25] B. Fermini, A.A. Fossa, The impact of drug-induced QT interval prolongation on drug discovery and development, *Nat. Rev. Drug Discov.* 2 (2003) 439–447.